Transmission of OCDM Based on Asymmetric Pair Mapping Over a Seven Core Fiber

Shuaidong Chen, Bo Liu [ID], Jianxin Ren [ID], Yaya Mao, Xiangyu Wu, Rahat Ullah [ID], Xiumin Song [ID], Yu Bai, Yibin Wan, Suiyao Zhu, Yongfeng Wu [ID], Lilong Zhao, and Tingting Sun

Abstract—**In this paper, transmission of orthogonal chirp division multiplexing (OCDM) based on asymmetric pair mapping over a seven core fiber is proposed. High-order 32 quadrature amplitude modulation (QAM) is reduced to quadrature phase-shift keying (QPSK) and 8 QAM signal employing asymmetric pair mapping, which will not affect the rate of the system. Combined with geometric shaping (GS), the average transmission power is successfully lowered, realizing signal damage suppression. In order to verify the performance of the proposed asymmetric pair mapping scheme, a 140 Gb/s asymmetric pair mapping OCDM signal transmission over 2 km seven core fiber is experimentally demonstrated. The experimental results show that the proposed transmission scheme has the best performance when the power distribution ratio (PDR) is 4 dB. Meanwhile, compared with GS 32 QAM with QPSK+rectangle 8 QAM, GS 32 QAM with QPSK+star 8 QAM and GS 32 QAM, the proposed asymmetric pair mapping OCDM signal has improved by 1.55 dB, 1.45 dB, and 0.7 dB, respectively. It has a wide range of applications in the future optical transmission system due to its outstanding performance in the suppression of high-order modulation signal degradation.**

Index Terms—**Geometric shaping, asymmetric pair mapping, signal reduced order.**

I. INTRODUCTION

THE global Internet traffic demand is increasing by the day due to the rapid development of new services such

Shuaidong Chen, Bo Liu, Jianxin Ren, Yaya Mao, Xiangyu Wu, Rahat Ullah, Yu Bai, Yibin Wan, Suiyao Zhu, Yongfeng Wu, Lilong Zhao, and Tingting Sun are with the Institute of Optics and Electronics, Jiangsu Key Laboratory for Optoelectronic Detection of Atmosphere and Ocean, Jiangsu International Joint Laboratory on Meteorological Photonics and Optoelectronic Detection, Nanjing University of Information Science & Technology, Nanjing 210044, China (e-mail: 1678612644@qq.com; bo@nuist.edu.cn; 003458@nuist.edu.cn; maoyy@nuist.edu.cn; 200029@nuist.edu.cn; rahat@nuist.edu.cn; baiyu1993 @126.com; 254547694@qq.com; 1095382021@qq.com; wuyongfeng@nuist .edu.cn; 001967@nuist.edu.cn; suntingting@nuist.edu.cn).

Xiumin Song is with the State Key Laboratory of Information Photonics and Optical Communications, Beijing Key Laboratory of Space-Ground Interconnection and Convergence, School of Electronic Engineering, Beijing University of Posts and Telecommunications, Beijing 100876, China (e-mail: xmsong@bupt.edu.cn).

as 8K video, Metaverse, and whole-house intelligence [1]. A series of researches on how to boost transmission capacity are currently underway to improve the transmission capacity of optical fiber communication systems and satisfy capacity demand. The recently proposed orthogonal chirp division multiplexing (OCDM) is a new type of multi-carrier transmission system, enabled by the digital signal process (DSP), which realizes the idea of high-speed data transmission by multiplexing a sequence of linear chirp waveforms [2]–[4]. Chirp signals are multiplexed and superposed in a way similar to orthogonal frequency division multiplexing (OFDM) [5]. It has been proved that the modulated chirps are orthogonal in the chirp dimension and do not interfere with each other during transmission [2]. In comparison to OFDM, OCDM is more resistant to the effects of channel fading and noise. The paper [6] confirms that the OCDM system outperforms OFDM in terms of anti-dispersion. The receiver sensitivity of the OCDM is 1.3 dB higher than that of the OFDM, according to our earlier research [7]. The conversion of classic low-order modulation formats like on-off keying (OOK) and quadrature phase-shift keying (QPSK) to high-order quadrature amplitude modulation (QAM) is also required due to the high transmission rate needed. High-order modulation improves the spectral efficiency of the system by carrying more bits in one symbol. It is currently the most direct and effective means to achieve high spectral efficiency. In addition, a greater modulation order demands a higher input optical power, which exacerbates nonlinear effects. Therefore, in a power-limited optical fiber communication system, the minimum Euclidean distance between the constellation points of the signal will decrease with the increase of the modulation order. It will reduce the receiver's tolerance for interference such as noise and dispersion, increasing the chances of the signal being misjudged. Geometric shaping (GS) [8] increases the minimum Euclidean distance between constellation points by redesigning the arrangement of constellation points, thereby reducing inter-symbol interference and improving the tolerance of noise. Generally speaking, when a constellation diagram is composed of a regular triangle or a regular hexagon as a unit cell, the Euclidean space can be fully utilized, and the minimum Euclidean distance between constellation points can be raised while maintaining the same transmit power. A GS structure based on asymmetric polygons is proposed. This asymmetric mapping structure improves the receiver sensitivity by 4 dB [9]. Therefore, the asymmetric mapping modulation in the future is also an effective way to reduce nonlinear damage.

Although the use of high-order modulation formats can effectively improve the transmission capacity of the system, the traditional single-mode fiber (SMF) transmission capacity is about to reach the Shannon limit [10]. After the dimensions of time, wavelength, polarization, and other dimensions are exhausted, researchers turn their attention to the space dimension. Spatial division multiplexing (SDM) technology utilizes fiber core and mode dimensions to improve transmission capacity [11]–[13]. Research on multi-core fibers, few-mode fibers, and hollow-core few-mode fibers has been a hot topic. In the 2012 ECOC, 1.01Pbit/s transmission was achieved through 12 core optical fiber, which is also the first time to achieve P-bit-level large-capacity optical signal transmission [14]. In 2020, 10.66 Pbit/s transmission based on 38-core 3-mode fiber was achieved, which is the maximum transmission rate reported so far [15]. It can be seen that SDM is an inevitable trend in the development of large-capacity optical transmission systems in the future. However, due to mode crosstalk in few-mode fibers, it is difficult to maintain the mode field in long-distance transmission, and the receiving end needs complex multiple in multiple out (MIMO) equalization processing, which makes it difficult to further increase the number of modes. The multi-core fiber uses the spatial dimension to set up multiple cores in one fiber, and the crosstalk between the cores is extremely low, which has attracted more attention. In our previous work, we successfully used the seven core fiber to achieve a 2 km transmission experiment. The results show that the isolation between the weakly coupled seven-core fibers is greater than 50 dB, and the bit error performance difference between the cores is less than 0.5 dB [16]–[17].

In this paper, we propose optical transmission of OCDM based on asymmetric pair mapping over a seven core fiber. The high-order 32 QAM constellation is reduced to low-order QPSK and 8 QAM through multi-power distribution. According to the distribution of the QPSK constellation, asymmetric constellation shaping is performed on the 8 QAM constellation. What's more, one-to-one correspondence between asymmetric GS 8 QAM and QPSK is designed for asymmetric pair mapping, which reduces the high transmitted power of the higher-order modulation format. The channel impairment of the higher-order modulation format can be suppressed, thus the transmission performance can be improved.

A 140 Gb/s seven core data transmission employing the proposed OCDM scheme for asymmetric pair mapping is successfully demonstrated in the experiment. Without loss of generality, the asymmetric pair mapping proposed in this paper is a novel coding modulation method based on digital signal processing regardless of the type of transmission system. It can be applied to transmission systems other than seven core fiber.

II. PRINCIPLES

The workflow of OCDM optical transmission based on asymmetric pair mapping proposed in this paper is shown in Fig. 1. The original data streams are mapped on QPSK and GS 8 QAM respectively according to the pair mapping. The two group symbols of asymmetric pair mapping are superimposed after loading high power density P1 and low power density P2
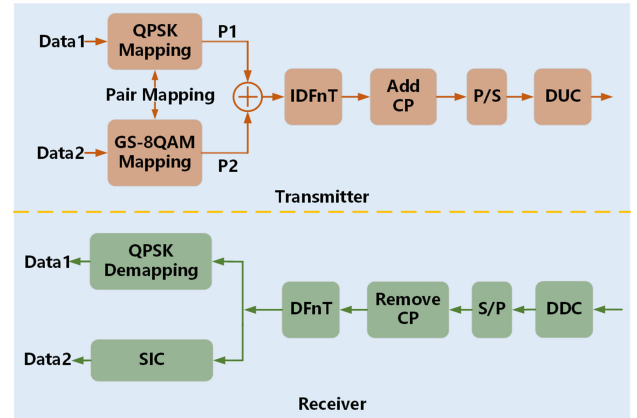

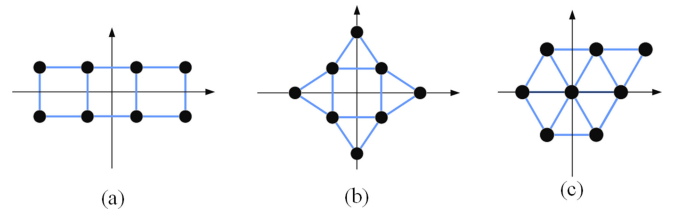Fig. 1. Workflow of OCDM optical transmission based on asymmetric pair mapping.

Fig. 2. Different structure of 8QAM((a) Rectangle 8QAM (b) Star 8QAM (c)GS 8 QAM).

respectively. Then inverse discrete Fresnel Transform (IDFnT) realizes OCDM modulation. A cyclic prefix (CP) is applied to alleviate inter-carrier interference (ICI) and inter-symbol interference (ISI) from the previous OCDM symbol. Finally, the original multicarrier data is converted into a serial signal by parallel-serial (P/S) conversion, and the complex signal is converted into a real number through Digital Up Conversion (DUC). After up-conversion, the real signal is transmitted in the seven core fiber. At the receiver end, data1 is recovered successively through Digital Down Conversion (DDC), serial-parallel (S/P) conversion, CP removal, DFnT, and QPSK demapping. Then, using the successive interference cancellation (SIC) algorithm, data 2 will be acquired.

32 QAM can be split into QPSK and 8 QAM. Fig. 2(a)-(b) shows two typical 8 QAM constellation structures. It has gradually evolved from the initial rectangular distribution to the star distribution. The GS 8 QAM used in this paper is based on the origin as the center, and is extended in an equilateral triangle to the outside. The constellation figure of merit (CFM) is an important indicator to measure a constellation diagram [8], which can be expressed as:

$$CFM\left(C\right) \triangleq d_{\min}^{2}\left(C\right)/P\left(C\right) \qquad (1)$$

Where $d_{\min}$ is the minimum Euclidean distance and $P(C)$ is the average transmit power. The CFM of three different structures of 8 QAM in Fig. 2 are 0.667, 0.8453 and 0.889, which indicates that GS 8 QAM has the best performance compared to the other two constellation distributions.
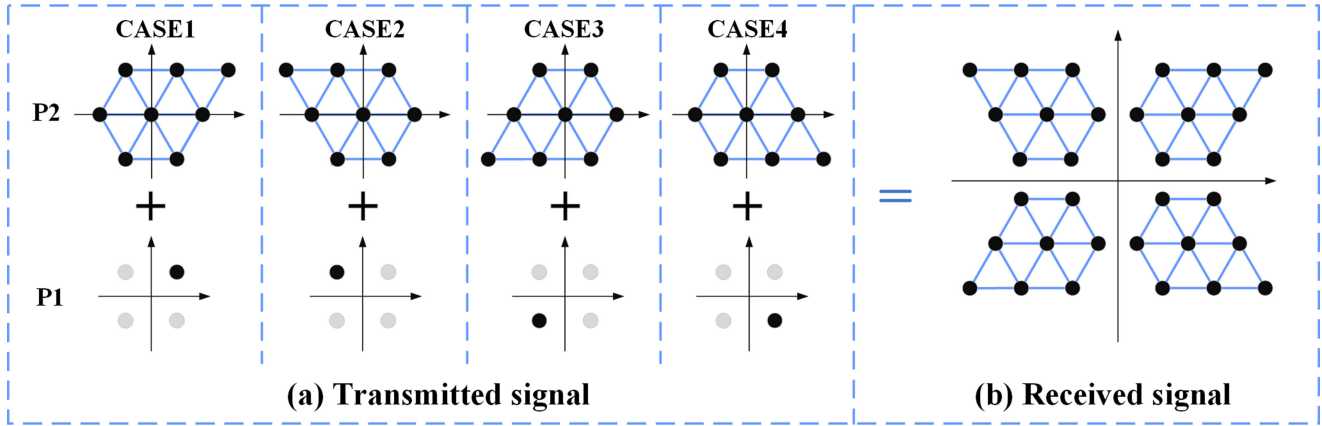
Fig. 3. Schematic diagram of asymmetric pair mapping.

A schematic of asymmetric pair mapping is shown in Fig. 3. The raw data is split into two parts, one part is used for QPSK mapping and the other part is utilized for GS 8 QAM mapping. However, the asymmetric constellation arrangement will lead to the overlap between the constellation points during the multi-power density superposition, which will affect the transmission performance of the system. Therefore, we design four GS 8 QAM constellations with different arrangements, corresponding to the constellations in the four quadrants of the QPSK signal respectively. Assuming that the QPSK signal is S_1 and the GS 8QAM signal is S_2, the superimposed signal of P1 and P2 after different power densities are allocated can be expressed as follows:

$$S = \sqrt{P_1}S_1 + \sqrt{P_2}S_2 \tag{2}$$

$$p_1 + p_2 = 1 \tag{3}$$

The superimposed constellation map is shown in Fig. 2(b). The overall constellation map is also an arrangement of 32 constellation points, but it has lower transmitting power compared with the traditional 32 QAM. We compare the transmitted signal power at different power density ratios (PDR) that can be expressed as:

$$PDR = P_1/P_2 \tag{4}$$

As can be observed from Table I, due to different power distribution, the low-power signal GS 8 QAM is distributed near the QPSK constellation, resulting in the low transmission power required. What's more, with the increase of PDR, the low-power signal is further decreased, and the required transmission power is constantly reduced as well. In order to ensure consistency with the standard 32QAM, we expand the original constellation points, that is, multiply by the corresponding optimal power coefficient. The optimal power coefficient in the Table I is the final minimum euclidean distance of GS 8 QAM with different PDR. For a standard 32

QAM constellation, the transmit power is 640. So, the optimal power coefficient can be express as $Optimal\ Power\ Coefficient = sqrt(640/power)$.

TABLE I
TRANSMITTING POWER OF DIFFERENT PDR

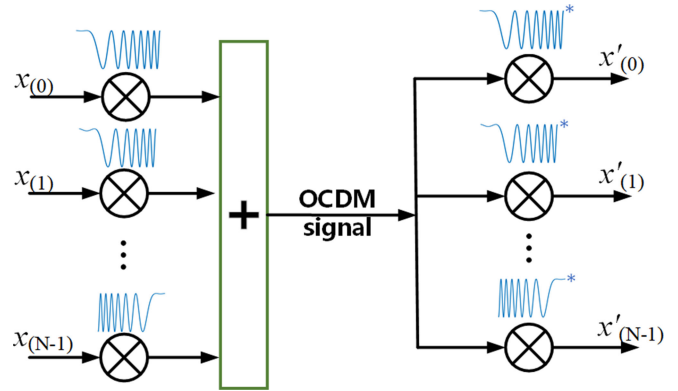| PDR	Power	Optimal Power Coefficient
2	79.2855	2.8411
3	77.5911	2.8720
4	76.3074	2.8961
5	75.3094	2.9152
6	74.5099	2.9307
7	73.8529	2.9438
8	73.3014	2.9548

Fig. 4. Schematic diagrams of the transceivers of OCDM.

The principle of OCDM is shown in Fig. 4. Different chirps modulate different signals. The baseband time-domain OCDM signal can be expressed as:

$$s(t) = \sum_{k=0}^{N-1} x(k)\psi_k(t), 0 \leq t \leq T \tag{5}$$

$$\psi_k(t) = \frac{1}{\sqrt{T}}e^{j\frac{\pi}{4}}e^{j\alpha\pi(t-k\Delta c)^2} \tag{6}$$
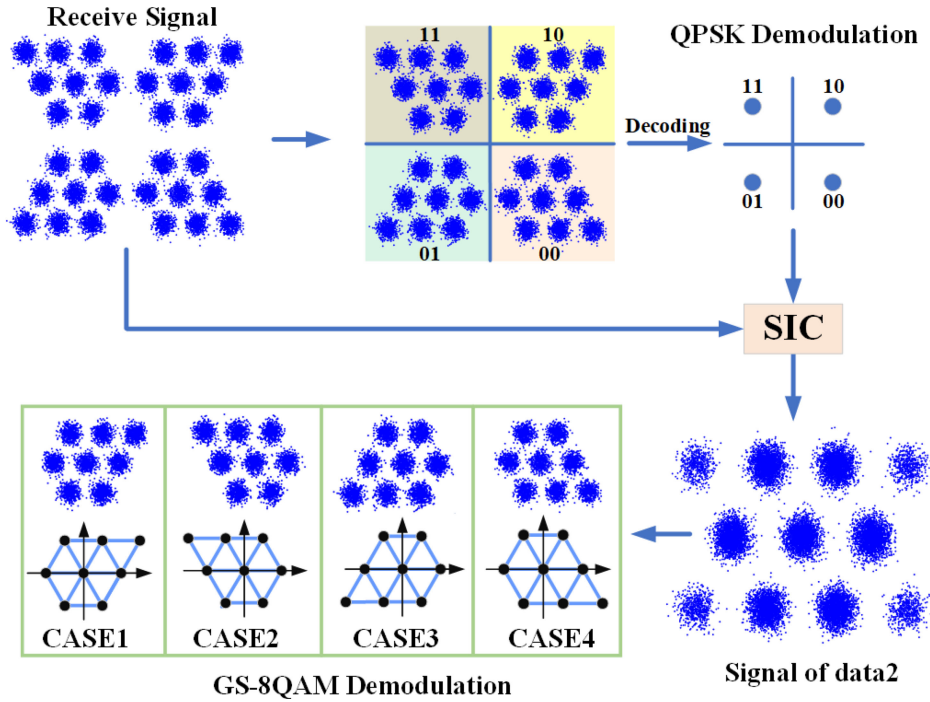
Fig. 5.   The principle of the demodelution at the receiver.

Where $\alpha = -N/T^2$ is the chirp rate and $\Delta c = T/N$ is the chirp shift of each chirp. It can be proved that the chirped signal in (6) has strict orthogonality.

$$\int \psi_{\mathrm{m}}^{*}(t)\psi_k(t)dt$$

$$= \int \frac{1}{\sqrt{T}}e^{j\frac{\pi}{4}}e^{-j\alpha\pi(t-m\Delta c)^2}\frac{1}{\sqrt{T}}e^{j\frac{\pi}{4}}e^{j\alpha\pi(t-k\Delta c)^2}dt$$

$$= \int_0^T e^{j\pi\frac{N}{T^2}(t-m\frac{T}{N})^2}e^{-j\pi\frac{N}{T^2}(t-k\frac{T}{N})^2}dt$$

$$= \delta(m-k) \tag{7}$$

Where m and k represent the m$^{\mathrm{th}}$ and k$^{\mathrm{th}}$ chirp respectively. From (7), it can be found that when $m \neq k$, the left side of the equation is always 0, thus ensuring the orthogonality between each chirp. If $m = k$, the signal can be demodulated at the receiver. Based on this characteristic, the demodulation of the chirped signal can be realized by the complex conjugate of the chirped signal.

In the digital domain, OCDM can be obtained by IDFnT as

$$s(n) = \frac{1}{\sqrt{T}}e^{j\frac{\pi}{4}}\sum_{k=0}^{N-1}x(k)$$

$$\times \left\{\begin{array}{l} e^{-j\frac{\pi}{N}(n-k)^2}\ \mathrm{N} \equiv 0(\mathrm{mod}2) \\[2mm] e^{-j\frac{\pi}{N}(n-k+\frac{1}{2})^2}\ \mathrm{N} \equiv 1(\mathrm{mod}2) \end{array}\right\} \tag{8}$$

Due to the orthogonality of each chirped signal, the demodulation of the OCDM signal can be realized by DFnT. According to (8), it can be found that the OCDM signal is complex and cannot be applied to the intensity modulation direct detection (IMDD) transmission system. DUC is performed to convert the complex baseband OCDM signal to passband so that all the spectral content is at the positive frequency while preserving all the information of the baseband signal [18]. Specifically, assuming that the continuous time domain signal after the P/S is $s(t)$, then the signal after the up-conversion can be given by:

$$S_P(t) = e^{j2\pi f_{up}t}s(t) \tag{9}$$

Among them f_{up} is the frequency of the up-conversion carrier. After up-conversion, the real part information of the signal can be expressed as:

$$S_\Re(\mathrm{t}) = \Re\{S_p(t)\}$$
$$= S_I(t)\cdot\cos 2\pi f_p t - S_Q(t)\cdot\sin 2\pi f_p t \tag{10}$$

$S_I(t)$ and $S_Q(t)$ respectively represent the inphase and quadrature components of the continuous time domain signal $s(t)$. This makes it possible to convert complex signals into real information that can be transmitted in IMDD without losing any useful information.

The receiving signal will be demodulated by DDC, S/P, CP removal, and DFnT. Fig. 5 is the schematic diagram showing the demodulation at the receiving end. The received constellation is consistent with the constellation point distribution in Fig. 3(b). The GS 8 QAM signal with low power is regarded as noise and the judgment is made in a different quadrant. The signals distributed in four different quadrants are demodulated as four constellation points of QPSK, so the data1 of high power density is easily demodulated. Based on SIC, the demodulated QPSK
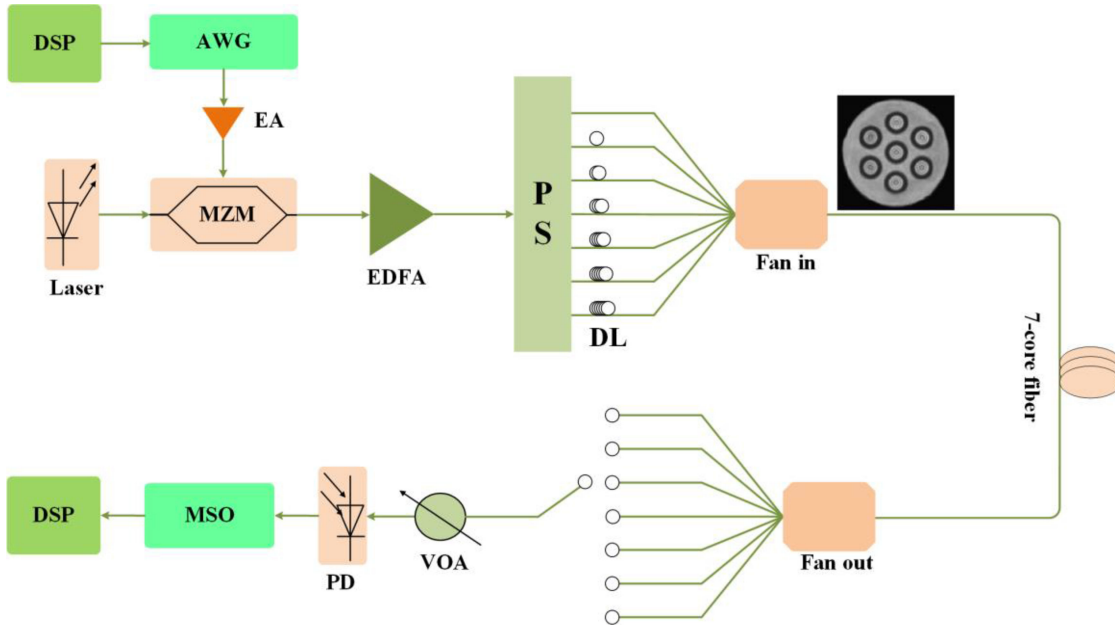
Fig. 6. Experimental setup (DSP: Digital signal process; AWG: Arbitrary waveform generator; EA: Electric amplifier; MZM: Mach-Zehnder modulator; EDFA: Erbium-doped fiber amplifier; DL: Delay line; PS: Power splitter: VOA: Variable optical attenuator; PD: Photodiode; MSO: Mixed signal oscilloscope).

signal will be re-modulated. Subtracting the QPSK signal from the receiving signal to get the data2 signal. The constellation points distribution of data 2 is shown in Fig. 5. The number of central constellation points and outer regular hexagon constellation points are significantly more than that of the outermost four constellation points. This is because, in the principle of asymmetric pair mapping, each group of cases will have the distribution of central and outer regular hexagon constellation points, while the four points on the edge corresponding to the unique constellation points in each case. Data2 can be recovered by demodulation based on the principle of asymmetric pair mapping.

III. Experimental Setup and Results

A. Experimental Setup

The experimental setup is shown in Fig. 6 for demonstrating the proposed OCDM asymmetric pair matching scheme. The data after DSP is loaded into an arbitrary waveform generator (AWG, TekAWG70002A) with 20 GSa/s for digital-to-analog conversion (DAC). A tunable laser, with a wavelength of 1550 nm and output power of 12 dBm, is used to generate continuous-wavelength (CW) lightwave signals. An electric amplifier (EA) is applied to amplify the radio frequency (RF) signal and then the electro-optic modulation is realized via a Mach-Zehnder modulator (MZM) with a bandwith of 40 GHz. To compensate for the insertion loss (IL) of the power splitter (PS) and energy loss of the link during the transmission, an Erbium-doped fiber amplifier (EDFA) is deployed to amplify the modulated optical signal. Then, the amplified signal is equally divided into seven parts by a PS, which are delayed separately by SMF for decorrelation. A fan in device realizes seven core multiplexing. The multiplexed
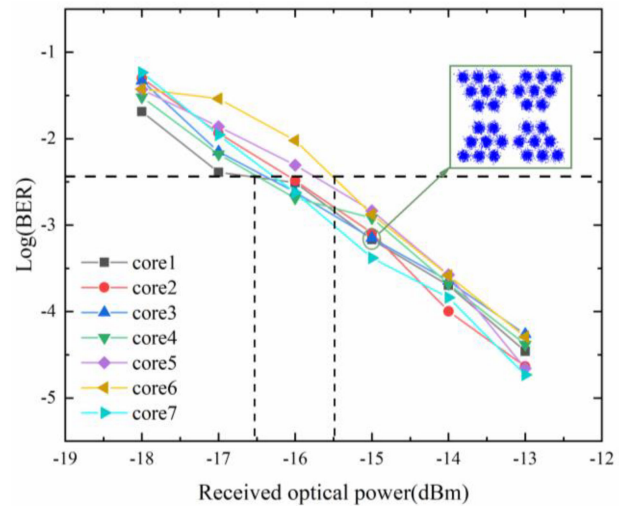

Fig. 7. BER performance of OCDM asymmetric pair matching signal in seven core fiber.

signal enters a 2 km weakly coupled seven core fiber for transmission. Another fan out device is installed at the receiver for demultiplexing. A variable optical attenuator (VOA) is applied to adjust the optical power. Photodiode (PD) which has a bandwith of 40 GHz is used for the detection and conversion of optical signals into electrical signals. The signal is received by a mixed signal oscilloscope (MSO, TekMSO73304DX) with a sampling rate of 50 GSa/s. Finally, offline DSP recovers the original data. We use DUC to convert the complex signal into a real number, so the transmission rate has nothing to do with the number of IFFT points. The number of subcarriers and the number of IFFT points are equal to 128. The total bit rate can be tantamount to the expression of (AWG sampling rate × entropy/ Up-sampling
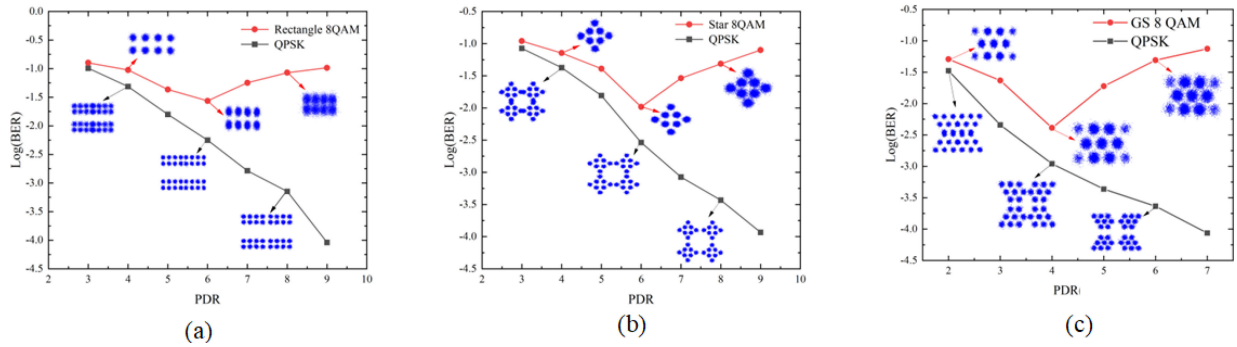
Fig. 8.   BER versus PDR of different 8QAM ((a) Rectangle 8QAM pair matching, (b) Star 8QAM pair matching, (c) GS 8QAM asymmetric pair matching).

coefficient /(1+CP)×number of core). In this experiment, the bit rate can be expressed as $20 \times 5/4/(1 + 1/4) \times 7 = 140\,\mathrm{Gb/s}$.

B. Experimental Results and Analysis

We tested the BER of signals in different cores to verify the transmission performance of the proposed OCDM asymmetric pair matching in seven core fiber. The BER performance gradually improves as the received optical power (ROP) increases, as seen in Fig. 7. This is because greater ROP values yielding a higher signal-to-noise ratio (SNR), resulting in a better receiver sensitivity. Each core's BER curves in the seven core fiber are also almost identical. At the hard-decision forward error correction (HD-FEC), BER limit of 3.8×10^{-3}, the best core 1 has a receiving power of -16.55 dBm, while the worst performance via core 6 has a receiving power of -14.45 dBm. The sensitivity difference between the two receivers is only 1.1dB. It shows that the seven core fiber used in this experiment has good uniformity and excellent transmission response.

At the receiver, data separation is performed from the received signal. The performance of the asymmetric pair mapping mainly depends on the allocated power weights. In order to obtain the best PDR, we tested the BER of rectangle 8 QAM, star 8 QAM and GS 8 QAM with different PDR. Fig. 8(a)–(c) shows the BER curves of three schemes. From Fig. 8, it can be found that with the increase of PDR, the power obtained by the QPSK signal in all schemes increases continuously, resulting in a gradual decrease in the BER of QPSK. Among these three schemes, the optimal PDR of rectangle 8 QAM and star 8 QAM is 6 and the optimal PDR of the proposed asymmetric pair mapping is 4. This is due to the in-phase signal and quadrature signal of rectangle 8 QAM and star 8 QAM is relatively large, so a large PDR is required to ensure that signals in different quadrants do not overlap. The asymmetric pair matching mapping scheme arranges the largest in-phase and quadrature components on the edge of each quadrant, which effectively avoids large PDR caused by excessive in-phase and quadrature components. A larger PDR will reduce the performance of the low-power signal allocated by data2, which will ultimately affect the overall performance of the signal. Moreover, the GS 8 QAM has the largest CFM, which is beneficial for the final constellation point decision. Therefore, when the three schemes all use their best PDR, the
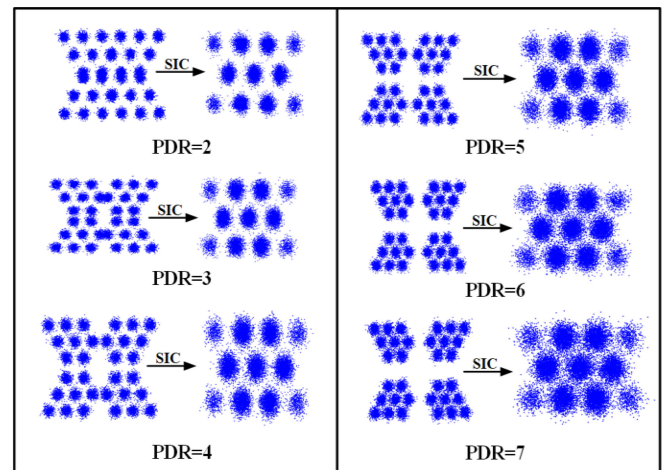

Fig. 9.   Constellation diagrams for OCDM asymmetric pair matching at different PDR.

BER of asymmetric pair mapping is the lowest. It can be seen from Fig. 8(c) that there is a dip in the BER curve of GS 8 QAM. This is because as the PDR increases, more power is allocated to QPSK. GS 8 QAM which can be seen as the interference is allocated to a very small power leading to the effect on QPSK is greatly reduced. After QPSK is restored, GS 8 QAM will be demodulated. GS 8 QAM needs to subtract QPSK from the received signal. Therefore, the performance of QPSK will affect the demodulation of GS 8 QAM. The error bits of QPSK are brought into the demodulation of GS 8 QAM, resulting in a high BER of GS 8 QAM even when the optical power is high. As the PDR increases, the error effect of QPSK decreases, and the BER of GS 8 QAM decreases gradually. When the PDR is higher, the performance of QPSK is further improved, but the power allocated in GS 8 QAM is lower, resulting in poor performance. Therefore, GS 8 QAM generally shows a trend of first decreasing and then increasing. There exists an optimal power ratio of 4 dB for the GS 8 QAM.

The experimental results in Fig. 8 are fully explained in Fig. 9. When the PDR is 2 dB or 3 dB, there is an overlap between the constellation points, which leads to error codes in the demodulation of data1 by the receiver. Because of the error propagation by the SIC algorithm, the BER of data2 is very high.
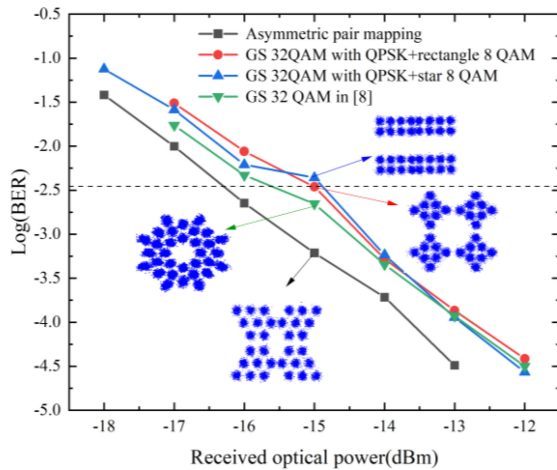
Fig. 10. BER comparison of different schemes.

When PDR is 4 dB, there is no overlap between the constellation points, and the constellation of data2 is relatively clear with good bit error performance. However, when PDR is greater than 5 dB, the distribution of constellation points to quadrant is more obvious, and the BER of data1 decreases. But the distribution of constellation points of data2 gets blurred, which affects the performance of data2 and all of the data.

To verify the superiority of the proposed asymmetric pair mapping, we compare this scheme with GS 32 QAM with QPSK+rectangle 8 QAM, GS 32 QAM with QPSK+star 8 QAM and GS 32 QAM in [8]. Fig. 10 is the BER comparison of different schemes. At the HD-FEC BER limit of 3.8×10^{-3}, the proposed asymmetric pair mapping scheme have sensitivity gains of 0.7 dB, 1.45 dB, and 1.55 dB, respectively when compared to GS 32 QAM in [8], GS 32 QAM with QPSK+star 8 QAM and GS 32 QAM with QPSK+rectangle 8 QAM. This is because the PDR of GS 32 QAM with QPSK+rectangle 8 QAM and GS 32 QAM with QPSK+star 8 QAM is 6, and the difference between the two channels is large, resulting in poor performance of low-power signals. The PDR of the asymmetric pair mapping is 4, the power difference between QPSK and GS 8 QAM is smaller, and the performance difference between the two sets of data is smaller, resulting in better overall transmission performance. Compared with GS 32 QAM in [8], the proposed asymmetric pair mapping method can perform channel equalization twice at the receiving end with SIC, which can more effectively compensate for channel impairments. And the minimum Euclidean distance of the asymmetric pair mapping is larger than that of GS 32QAM which leading a better performance.

IV. CONCLUSION

In this paper, we propose an OCDM optical transmission scheme based on asymmetric pair mapping. High power QPSK signal and low power GS 8 QAM are integrated into high order 32 QAM signal for transmission through asymmetric pair matching. The signal is demodulated by the SIC algorithm at the receiver. We experimentally demonstrated 140 Gb/s pair matching OCDM signal transmission over 2 km seven core fiber. The suggested asymmetric pair mapping improves the receiving end sensitivity by 0.7dB, 1.45dB, 1.55dB when compared to GS 32 QAM, GS 32 QAM with QPSK+star 8 QAM and GS 32 QAM with QPSK+rectangle 8 QAM. We believe that this approach can be used to effectively improve high-order modulation signals performance in future high-capacity optical transmission systems.

REFERENCES

[1] X. Xu et al., "A robust probabilistic shaping PON based on symbol-level labeling and rhombus-shaped modulation," *Opt. Exp.*, vol. 26, no. 20, pp. 26576–26589, 2018.

[2] X. Ouyang and J. Zhao, "Orthogonal chirp division multiplexing," *IEEE Trans. Commun.*, vol. 64, no. 9, pp. 3946–3957, Sep. 2016.

[3] X. Ouyang, C. Antony, J. Zhao, G. Talli, and P. D. Townsend, "Intensity-modulation direct-detection OCDM system based on digital up-conversion," in *Proc. Conf. Lasers Electro.-Opt.*, 2018, pp. 1–2.

[4] X. Ouyang, G. Talli, M. Power, and P. D. Townsend, "Iterative block decision feedback equalization for IM/DD-based OCDM to compensate chromatic-dispersion-induced power fading," *J. Lightw. Technol.*, vol. 37, no. 17, pp. 4349–4358, Sep. 2019.

[5] J. Armstrong, "OFDM for optical communications," *J. Lightw. Technol.*, vol. 27, no. 3, pp. 189–204, Feb. 2009.

[6] X. Ouyang and J. Zhao, "Orthogonal chirp division multiplexing for coherent optical fiber communications," *J. Lightw. Technol.*, vol. 34, no. 18, pp. 4376–4386, Sep. 2016.

[7] L. Yuan et al., "High-security OCDM-PON system of 7-core fiber based on CFCM encryption," *Opt. Lett.*, vol. 47, no. 1, pp. 186–189, 2022.

[8] J. Ren et al., "A probabilistically shaped star-CAP-16/32 modulation based on constellation design with honeycomb-like decision regions," *Opt. Exp.*, vol. 27, no. 3, pp. 2732–2746, 2019.

[9] X. Wu et al., "A probabilistic shaping method based on intrinsic bit-level labeling and asymmetric polygon modulation for optical interconnects," *Opt. Commun.*, vol. 444, pp. 68–73, 2019.

[10] C.E. Shannon, "The mathematical theory of communication," *M D Comput.*, vol. 14, no. 4, pp. 306–317, 1997.

[11] G. Rademacher et al., "Long-haul transmission over few-mode fibers with space-division multiplexing," *J. Lightw. Technol.*, vol. 36, no. 6, pp. 1382–1388, Mar. 2018.

[12] K. Shibahara et al., "DMD-unmanaged long-haul SDM transmission over 2500-km 12-core × 3-mode MC-FMF and 6300-km 3-mode FMF employing intermodal interference cancelling technique," in *Proc. Opt. Fiber Commun.*, 2018, Paper Th4C.6.

[13] R. Ryf et al., "Coupled-core transmission over 7-core fiber," in *Proc. Opt. Fiber Commun.*, 2019, Paper Th4B.3.

[14] H. Takara et al., "1.01-Pb/s (12 SDM/222 WDM/456 Gb/s) crosstalk managed transmission with 91.4-b/s/Hz aggregate spectral efficiency," in *Proc. Eur. Conf. Exhib. Opt. Commun.*, 2012, Paper Th3C.1.

[15] G. Rademacher et al., "10.66 peta-bit/s transmission over a 38-core-three-mode fiber," in *Proc. Opt. Fiber Commun.*, 2020, Paper Th3H.1.

[16] J. Zhang et al., "Enhanced 3D-CAP modulation with information-inserted time slots for seven-core fiber transmissions," *Opt. Exp.*, vol. 28, no. 17, pp. 24991–24999, 2020.

[17] S. Chen et al., "A 7D cellular neural network based OQAM-FBMC encryption scheme for seven core fiber," *J. Lightw. Technol.*, vol. 39, no. 22, pp. 7191–7198, Nov. 2021.

[18] X. Ouyang, G. Talli, M. Power, and P. Townsend, "Orthogonal chirp-division multiplexing for IM/DD-based short-reach systems," *Opt. Exp.*, vol. 27, no. 16, pp. 23620–23632, 2019.